MECHANISMS OF SIGNAL TRANSDUCTION:

Polarized Expression of G Protein-coupled Receptors and an All-or-None Discharge of Ca^{2+} Pools at Initiation Sites of $[Ca^{2+}]_i$ Waves in Polarized Exocrine Cells

Dong Min Shin, Xiang Luo, Thomas M. Wilkie, Laurence J. Miller, Ammon B. Peck, Michael G. Humphreys-Beher and Shmuel Muallem

J. Biol. Chem. 2001, 276:44146-44156.
doi: 10.1074/jbc.M105203200 originally published online September 11, 2001

THE JOURNAL OF BIOLOGICAL CHEMISTRY
Vol. 276, No. 47, Issue of November 23, pp. 44146–44156, 2001
Printed in U.S.A.

Polarized Expression of G Protein-coupled Receptors and an All-or-None Discharge of Ca^{2+} Pools at Initiation Sites of $[Ca^{2+}]_i$ Waves in Polarized Exocrine Cells*

Received for publication, June 6, 2001, and in revised form, August 28, 2001
Published, JBC Papers in Press, September 11, 2001, DOI 10.1074/jbc.M105203200

Dong Min Shin‡, Xiang Luo‡, Thomas M. Wilkie§, Laurence J. Miller¶, Ammon B. Peck‖, Michael G. Humphreys-Beher, and Shmuel Muallem‡ ‡‡**

*From the Departments of ‡Physiology and §Pharmacology, University of Texas Southwestern Medical Center, Dallas, Texas 75390, the ¶Center for Basic Research in Digestive Diseases, Mayo Clinic and Foundation, Rochester, Minnesota 55905, the ‖Department of Pathology and Laboratory Medicine and the **Departments of Oral Biology and Pharmacology and Therapeutics, University of Florida, Gainesville, Florida 32610*

In the present work we examined localization and behavior of G protein-coupled receptors (GPCR) in polarized exocrine cells to address the questions of how luminal to basal Ca^{2+} waves can be generated in a receptor-specific manner and whether quantal Ca^{2+} release reflects partial release from a continuous pool or an all-or-none release from a compartmentalized pool. Immunolocalization revealed that expression of GPCRs in polarized cells is not uniform, with high levels of GPCR expression at or near the tight junctions. Measurement of phospholipase Cβ activity and receptor-dependent recruitment and trapping of the box domain of RGS4 in GPCRs complexes indicated autonomous functioning of G_q-coupled receptors in acinar cells. These findings explain the generation of receptor-specific Ca^{2+} waves and why the waves are always initiated at the apical pole. The initiation site of Ca^{2+} wave at the apical pole and the pattern of wave propagation were independent of inositol 1,4,5-trisphosphate concentration. Furthermore, a second Ca^{2+} wave with the same initiation site and pattern was launched by inhibition of sarco/endoplasmic reticulum Ca^{2+}-ATPase pumps of cells continuously stimulated with sub-maximal agonist concentration. By contrast, rapid sequential application of sub-maximal and maximal agonist concentrations to the same cell triggered Ca^{2+} waves with different initiation sites. These findings indicate that signaling specificity in pancreatic acinar cells is aided by polarized expression and autonomous functioning of GPCRs and that quantal Ca^{2+} release is not due to a partial Ca^{2+} release from a continuous pool, but rather, it is due to an all-or-none Ca^{2+} release from a compartmentalized Ca^{2+} pool.

Ca^{2+} signaling by G protein-coupled receptors (GPCR)[1] involves the generation of inositol 1,4,5-trisphosphate (IP_3) in the cytosol and Ca^{2+} release from the endoplasmic reticulum (1). In polarized exocrine cells, Ca^{2+} release is not uniform but occurs in the form of Ca^{2+} waves. Rooney *et al.* (2) reported a unique initiation site and propagation pattern of GPCR-evoked Ca^{2+} waves in hepatocytes. Kasai *et al.* (3) first described the unique feature of initiation of Ca^{2+} waves at the apical pole and their propagation to the basal pole of pancreatic acini. This phenomenon was later confirmed in pancreatic acinar cells (3–6) and was extended to other exocrine cells (7, 8). Subsequent studies showed that expression of high levels of all IP_3 receptor (IP_3Rs) isoforms at the apical pole accounts for the initiation of Ca^{2+} waves at this site (7, 9). Furthermore, the apical pole showed higher sensitivity to Ca^{2+} release by IP_3 than other regions of the cell, including the basal pole (3, 10, 11). However, since the discovery of the polarized Ca^{2+} waves in exocrine cells, it remained a mystery how IP_3 can be generated in the apical pole to initiate the waves. Early functional (12) and radioligand (13) localization of receptors in tissue slices indicated that GPCRs are expressed in the basal membrane. Therefore, it was assumed that during GPCR stimulation IP_3 generated in the basal pole diffuses to the apical pole to initiate Ca^{2+} release and waves (14). This assumption has several difficulties. For example, at maximal stimulus intensity Ca^{2+} release starts within few milliseconds of cell stimulation. The diameter of exocrine acinar cells is about 20 μm. This requires exceptionally high rate of diffusion of IP_3 in the cytosol of this cells. In pancreatic acini, Ca^{2+} release events can remain confined to the apical pole (3, 4). This requires continuous traffic of IP_3 through the cytosol without causing Ca^{2+} release. Another alternative is generation of IP_3 in or close proximity to the apical pole. This requires localization of GPCR at the apical pole. With the development of suitable antibodies for immunolocalization of GPCR and the use of isolated cell clusters that increase the resolution of immunolocalization, it became possible to re-examine GPCR localization in relation to initiation of Ca^{2+} waves.

Another aspect of Ca^{2+} release in terms of initiation and propagation of Ca^{2+} waves is the architecture of the Ca^{2+} pool and the dynamics of Ca^{2+} release. Propagation of Ca^{2+} waves requires either sequential Ca^{2+} release from a compartmentalized pool or release from different sections of a continuous pool along the path of the Ca^{2+} wave. A unique property of Ca^{2+} release from internal stores, the quantal feature of Ca^{2+} release (15), can reflect the spatial organization of the Ca^{2+} pool that is needed for propagation of Ca^{2+} waves. Ca^{2+} release evoked by either stimulation of GPCR (15), activation of the IP_3

* The costs of publication of this article were defrayed in part by the payment of page charges. This article must therefore be hereby marked "*advertisement*" in accordance with 18 U.S.C. Section 1734 solely to indicate this fact.

‡‡ To whom correspondence should be addressed: the University of Texas Southwestern Medical Center, Dallas, 5323 Harry Hines Blvd., Dallas, TX 75390-9040. Tel.: 214-648-2593; Fax: 214-648-8879; E-mail: SHMUEL.MUALLEM@utsouthwestern.edu.

[1] The abbreviations used are: GPCR, G protein-coupled receptors; IP_3, inositol 1,4,5-trisphosphate; IP_3R, IP_3 receptor(s); SERCA, sarco/endoplasmic reticulum Ca^{2+}-ATPase; PLC, phospholipase C; M3R, muscarinic type 3 receptor; Ab, antibody; mAb, monoclonal antibody; pAb, polyclonal antibody; CCK, cholecystokinin; BS, bombesin; CCK, CCK receptor(s); Tg, thapsigargin.

receptors (15–17), or activation of the ryanodine receptors (18) has quantal properties, that is at submaximal stimulus intensity only part of the Ca^{2+} pool is released and at increased stimulus an increased fraction of the pool is released. Two main models were proposed to explain quantal release. The first is an all-or-none release of Ca^{2+} from a compartmentalized pool that has a continuum of sensitivity to IP_3 (15, 19, 20). The second model proposes phasic Ca^{2+} release from a homogeneous pool where the phase of release at a given IP_3 concentration is determined by gating of IP_3Rs activity by Ca^{2+} content remaining in the stores (21). The first model fits well with the experimentally observed variable sensitivity of different cellular regions of pancreatic acini to IP_3-mediated Ca^{2+} release (3, 11). On the other hand, recent work (22) in *Xenopus* oocytes reports that the quantal behavior of Ca^{2+} release stems from rapid adaptation of the IP_3R channels of a continuous Ca^{2+} pool and claimed to refute the compartmentalization model.

The constancy of initiation of Ca^{2+} waves in the apical pole by all GPCR of pancreatic acini and the variable sensitivity of different cellular regions to IP_3-mediated Ca^{2+} release prompted us to determine localization of GPCR in pancreatic acini and to examine their autonomous behavior and what mechanism they use to evoke quantal release. We report that expression of GPCR is highly enriched in the apical pole, at or just underneath the tight junctions. This provides an explanation of how Ca^{2+} waves are initiated at the apical pole. The initiation site and propagation pattern of Ca^{2+} waves are receptor-specific in the same cells. This appears to be the result of autonomous coupling of receptors to G proteins and thus operation of GPCR signaling complexes. Finally and most notably, by using agonist concentration jump protocols and inhibition of the sarco/endoplasmic reticulum Ca^{2+}-ATPase (SERCA) pump of partially stimulated cells, we provide evidence that the quantal properties of Ca^{2+} release are due to an all-or-none Ca^{2+} release from a compartmentalized Ca^{2+} pool.

EXPERIMENTAL PROCEDURES

Materials—Thapsigargin was from Alexis. The anti-muscarinic monoclonal antibody (mAb) M35 was from Argene. The hybridoma cells producing the 5H9 mAb against muscarinic type 3 receptor (M3R) and the specificity of the Abs were described elsewhere (23). Two pAbs that recognize different epitopes of the cholecystokinin (CCK) receptor were prepared using peptide antigens, and their specificity was extensively characterized and verified by blocking with peptides that were used to raise the anti-CCKR antibodies (24). A recombinant M2R was a generous gift from Dr. Eliott Ross (University of Texas Southwestern Medical Center, Dallas). Anti-IP_3R2 pAb was a generous gift from Dr. Akihiko Tanimura (University of Hokkaido, Ishikari-Tobetsu, Japan). The box domain of RGS4 (4Box) was prepared as described (25). Anti-IP_3R3 mAb and anti ZO1 pAbs were purchased from ABR and Zymed Laboratories Inc., respectively. Anti-ZO1 mAb was obtained from the Hybridoma Bank at the University of Iowa.

Preparation of Pancreatic Acini and Single Acinar Cells—Acini were prepared from the pancreas of 100–150-g rats by limited collagenase digestion as described previously (6). After isolation, the acini were resuspended in a standard solution A containing (in mM) 140 NaCl, 5 KCl, 1 $MgCl_2$, 1 $CaCl_2$, 10 Hepes (pH 7.4 with NaOH), 10 glucose, and 0.1% bovine serum albumin and kept on ice until use. Doublet or triplet acinar cell clusters were obtained by incubation of a minced pancreas in a 0.025% trypsin, 0.02% EDTA solution for 5 min at 37 °C. After washing with solution A supplemented with 0.02% soybean trypsin inhibitor, doublets and triplets were liberated by a 7-min incubation at 37 °C in the same solution that also contained 160 units/ml pure collagenase. The cells were washed with solution A and kept on ice until use.

$[Ca^{2+}]_i$ Imaging—Pancreatic acinar cells were loaded with Fura 2, and $[Ca^{2+}]_i$ was imaged as detailed before (6). Fura 2 fluorescence was measured at a single excitation wavelength of 380 nm, by averaging eight consecutive images for each time point. Under these conditions and using a frame size of 256 × 240 pixels, recording was at a resolution of 90 ms/averaged image. During perfusion with the control solution and just before the first stimulation, the image of resting cells was acquired and was taken as the fluorescence signal at time 0 (F_0). Pixel values of all subsequent images were divided by this image, and the traces and images are the calculated F_t/F_0, where F_t is the fluorescence at time t.

To calculate the distance between initiation sites from which Ca^{2+} waves were triggered by different agonists or sequential application of the same agonist in the same cell, the initiation sites of all waves were marked on the first image, and the image was transferred to Adobe Photoshop. A right triangle was drawn using the ray between the two initiation sites as the hypotenuse. The x and y axes originated from the left and top plane, respectively. The distance between the initiation sites was then calculated by means of the Pythagorean theorem. The distances from multiple experiments were averaged and are given as means ± S.E. Although this procedure allowed quantitative analysis of the distance between initiation sites, such analysis has limitations inherent to the imaging procedure. The most critical limitation is the spatial resolution of cell imaging. The initiation sites and the waves are three-dimensional, whereas imaging at a speed needed to capture Ca^{2+} waves can be done only in two dimensions. Another limitation of the measurement is the temporal resolution of our recording system. This resulted in initiation sites that occupy 1–2 μm^2. Nevertheless, the differences in Ca^{2+} wave initiation sites and propagation pattern observed when cells were stimulated with two different agonists were sufficiently large to allow quantitative analysis of our measurements.

Electrophysiology—The whole cell configuration of the patch clamp technique was used for measurement of Ca^{2+}-activated Cl^- current, which correlates with changes in $[Ca^{2+}]_i$ near the plasma membrane (26). The experiments were performed with single acinar cells perfused with solution A. The standard pipette solution contained the following (in mM): 140 KCl, 1 $MgCl_2$, 0.5 EGTA, 5 ATP, 10 Hepes (pH 7.3 with KOH) with or without 100 nM 4Box, as described in previous studies (27). The 4Box was dialyzed against an ATP-free pipette solution and concentrated to about 5 μM with a centricone system. Seals of 6–10 gigohms were produced on the cell membrane, and the whole cell configuration was obtained by gentle suction or voltage pulses of 0.5 V for 0.3–1 ms. The patch clamp output (Axopatch-1B, Axon Instruments) was filtered at 20 Hz. Recording was performed with patch clamp 6 and a Digi-Data 1200 interface (Axon Instruments). All traces shown were recorded at a holding potential of −40 mV.

Measurement of IP_3—IP_3 levels were measured by a radioligand assay as described elsewhere (28). Acini in solution A were stimulated with the indicated combination of agonists for 10 s at 37 °C. The reactions were stopped by addition of 20 μl of ice-cold 20% perchloric acid to 200 μl of samples, vigorous mixing, and incubation on ice for at least 10 min to allow precipitation of proteins. The supernatants were collected and transferred to clean tubes. Standards of IP_3 were prepared in the same manner. The perchloric acid was removed and IP_3 extracted by the addition of 0.15 ml of Freon and 0.15 ml of tri-*n*-octylamine. IP_3 content in the aqueous phase was measured by displacement of $[^3H]IP_3$ using microsomes prepared from bovine brain cerebella (28).

Immunocytochemistry—The immunostaining procedure was described previously (29). In brief, cells attached to glass coverslips were fixed and permeabilized with cold methanol. After removal of methanol, nonspecific sites were blocked by a 1-h incubation in blocking medium prior to incubation with 50 μl of blocking medium containing control serum (controls) or the following antibodies: 1:500 dilution of the M35 mAb that recognizes all muscarinic receptors; the same mAbs that were reabsorbed with recombinant M2R; 1:250 dilution of the 5H9 mAb recognizing the M3R; 1:200 dilution of pAb specific for the M3R; 1:50 dilution of pAb1 and a 1:100 dilution of pAb2 that recognize the CCK receptor; 1:200 dilution of mAb against IP_3R3; 1:100 dilution of pAb against IP_3R2; 1:20 dilution of mAb against ZO1; and 1:100 dilution of pAb recognizing ZO1. After incubation with the various primary antibodies overnight at 4 °C, the cells were washed three times with the incubation buffer. For the experiment with the 5H9 mAbs in Fig. 4*A*, two different protocols were used. The first was a standard protocol using permeabilized cells. Under these conditions, all pools of M3R were detected. Because this antibody recognizes an extracellular epitope of the M3R diagnostic of Sjögren syndrome (23), it was used to label the receptors in the plasma membrane by incubating a 0.5-ml suspension of intact cells with 50 μl of 5H9 mAb for 30 min at 37 °C. The cells were then washed 3 times with phosphate-buffered saline to remove excess antibodies before fixation with 0.5 ml of cold methanol. All steps post-fixation were the same as with permeabilized cells. The primary Abs were detected with goat anti-rabbit or anti-mouse IgG tagged with fluorescein or rhodamine. Images were collected with a Bio-Rad MRC 1024 confocal microscope.

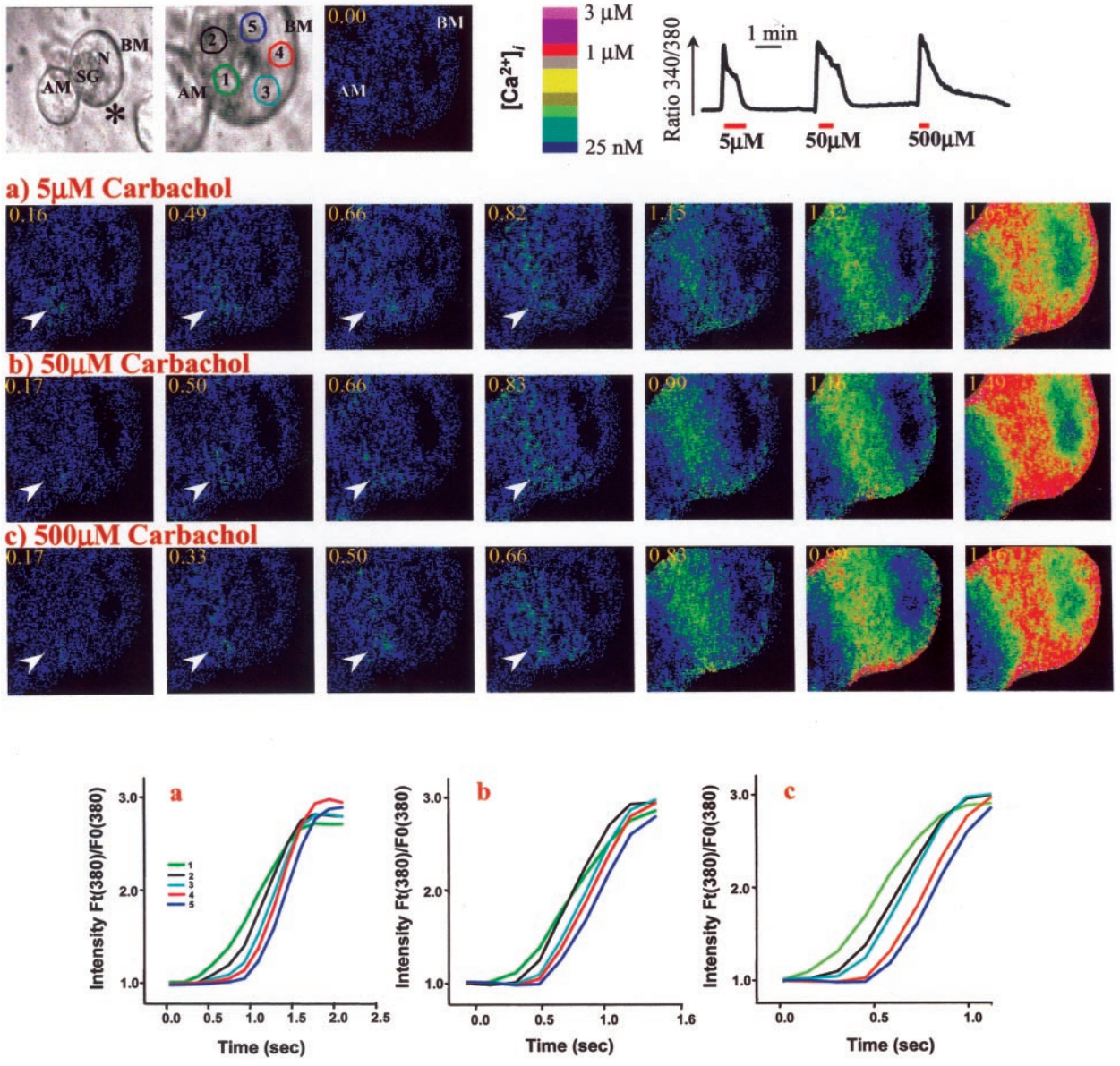

FIG. 1. **Ca^{2+} wave initiation site and pattern are independent of $[IP_3]$.** Fura 2-loaded doublet or triplet cell clusters were stimulated with 5, 50, and 500 μM carbachol. The cells were perfused with solution A for 3 min between the stimulations. The *top left* bright field image is × 600 magnification and the *middle* image is × 1000 magnification of the cell marked by an *asterisk*. The *top right* image shows the Fura 2 ratio under resting conditions. The first image in each row shows the first detected $[Ca^{2+}]_i$ increase by the respective carbachol concentration. The *arrowheads* mark the exact same spot in each image, demonstrating the same initiation site at all carbachol concentrations. The sequential images show the identical Ca^{2+} wave patterns at all carbachol concentrations. The *bottom panel* show the changes in F_t/F_0 ratios during the $[Ca^{2+}]_i$ rise phase for the three carbachol concentrations. *Traces 1–5* show the $[Ca^{2+}]_i$ changes in the areas marked *1–5* in the bright-field image. Please note the different times at *top left* of each sequence of images and the different time scales for the traces at each agonist concentration, demonstrating the effect of increased agonist concentration on the speed of the wave. *AM*, apical membrane; *BM*, basal membrane; *SG*, secretory granule; *N*, nucleus.

RESULTS

Receptor-specific Ca^{2+} Waves—Repetitive stimulation of pancreatic acinar cells with the same high concentration of agonist evokes Ca^{2+} waves with the same initiation site and propagation pattern (6). The quantal properties of agonist-mediated Ca^{2+} release (15) raised the question of whether partial and maximal discharge of the pool generates the same or different Ca^{2+} waves. In particular, it was of interest to determine whether the wave initiates from the same site at low and high IP_3 concentrations generated by weak and intense agonist stimulation. The properties of Ca^{2+} waves evoked by repetitive, brief stimulation with increasing concentration of agonist (5, 50, and 500 μM carbachol) are depicted in Fig. 1. Similar results were obtained in seven different cell preparations. All experiments were performed with clusters of doublet or triplet cells to ensure polarized expression of signaling protein was maintained. The *arrowheads* in the first image of each series show that the initiation site is constant and is independent of the IP_3 concentration used to initiate the wave. The calculated distance between initiation sites (see "Experimental Procedures") averaged 0.19 ± 0.05 μm (n = 7). The diameter of an acinar cell was about 20 μm. In addition, the pattern of wave propagation remained constant at all agonist concentrations. Increased stimulation intensity only increased the rate of Ca^{2+} wave propagation.

Constant initiation site and propagation patterns of Ca^{2+} waves were also observed with repetitive stimulation of another GPCR, the CCK receptor (see below). However, in previous work (6) we reported that stimulations of multiple GPCRs in the same rat pancreatic acinar cell evoked receptor-specific

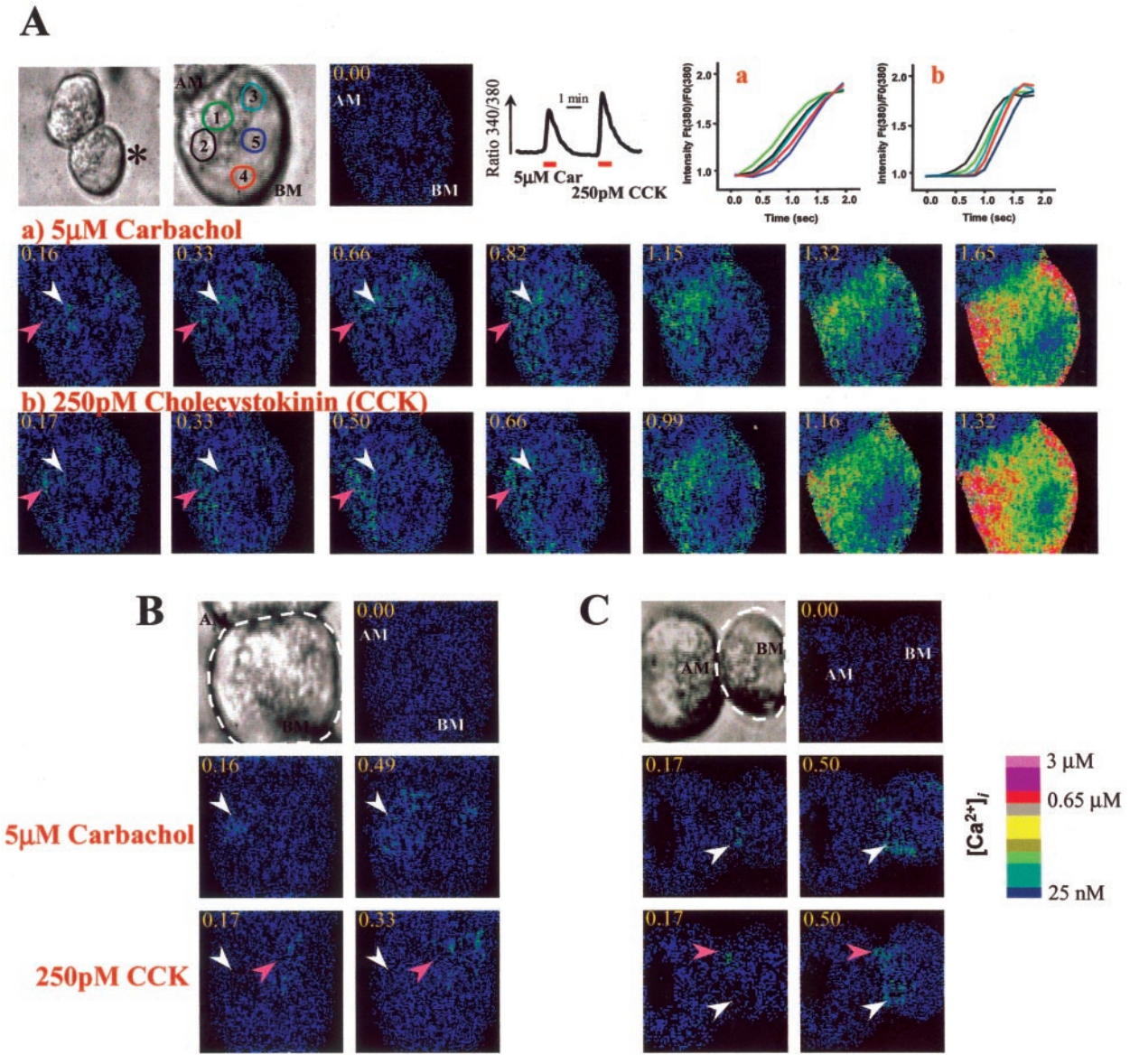

FIG. 2. **Receptor-specific initiation site and propagation pattern of Ca^{2+} waves.** Cells were sequentially stimulated with 5 μM carbachol and 0.25 nM CCK, as indicated in the *traces* in the *upper panel*. *A* shows the initiation site and pattern of the Ca^{2+} wave evoked by activation of the two receptors in the same cell. *B* and *C* show additional examples of the different Ca^{2+} wave initiation sites evoked by carbachol (*white arrowhead*) and CCK (*magenta arrowhead*) stimulation in the same cells. *AM*, apical membrane; *BM*, basal membrane.

Ca^{2+} waves in terms of initiation sites and propagation patterns. Cancela *et al.* (30) used mouse pancreatic acinar cells to suggest that Ca^{2+} waves are stochastic and are similar for all GPCRs in a given cell. Therefore, we examined Ca^{2+} waves evoked by carbachol and CCK stimulation in the same cell of small acinar clusters. Fig. 2 shows three examples of five experiments with similar results. The cells were stimulated with submaximal agonist concentrations to increase the temporal resolution of the waves. The *white* (carbachol) and *magenta* (CCK) *arrowheads* in the first image of each experiment show that, without exception, the initiation site of Ca^{2+} waves was different between the two agonists. The calculated distance between the carbachol and CCK initiation averaged 4.5 ± 1.5 μm (range 1.2–9.1 μm, $n = 5$). Although the waves initiated by stimulation of the two receptors propagated along the cell periphery, differences in wave patterns were noticeable in most experiments. Close examination of the results in Fig. 5*A* of Cancela *et al.* (30) also show that in a single isolated mouse pancreatic acinar cell activation of the muscarinic and CCK receptors resulted in different initiation sites of Ca^{2+} waves. This is particularly evident when the third image of the acetylcholine series is compared with the second image of the CCK series. The Ca^{2+} waves evoked by the two GPCRs had different spatial propagation pattern.

Autonomous Behavior of Signaling Complexes—The constancy of Ca^{2+} waves evoked by repetitive stimulation of the same GPCR, their independence of stimulus intensity, and the different Ca^{2+} wave evoked by activation of different GPCRs in the same cell suggest autonomous functioning of GPCRs. We used two experimental protocols to test this prediction. In the first set of experiments we examined IP_3 production by maximal agonist concentrations added individually or in combination. Although maximal stimulation of each of the GPCRs can mobilize the entire Ca^{2+} pool (see below), Fig. 3*A* shows that all combinations of agonists produced a nearly additive increase in IP_3 concentration. Hence, each GPCR can activate different pools of cellular PLCβ or distinct portions of a single pool that is in excess to the total number of GPCRs.

In the second protocol we used the RGS domain of RGS4 (4Box) to demonstrate autonomous functioning of the GPCRs

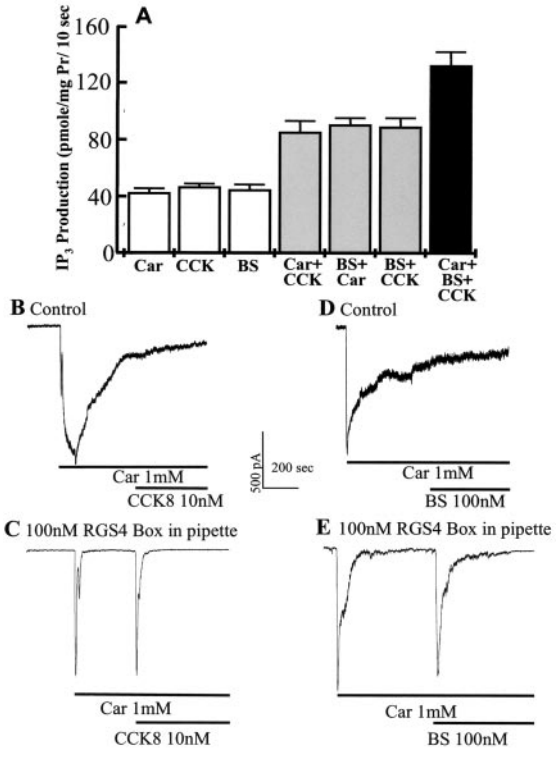

FIG. 3. **Autonomous behavior of GPCR complexes.** *A* shows stimulation of IP_3 production by 1 mM carbachol (*Car*), 10 nM CCK8b, and 100 nM BS alone (*open column*) and combinations of two (*gray columns*) or the three agonists (*filled column*). *B–E* show the Ca^{2+}-activated Cl^- current recorded from control cells or cells dialyzed with 100 nM 4Box for 7 min before the first stimulation. The *bars* indicate where the cells were stimulated with the indicated agonist concentration. Note that CCK8 and BS had no effect on $[Ca^{2+}]_i$ in carbachol-stimulated cells under control conditions but evoked a maximal response in cells dialyzed with 4Box.

in the same cell. The 4Box lacks receptor recognition domain and is a poor inhibitor of signaling in resting cells (31). The 4Box binds to activated α-subunits of G proteins (25, 32) and is nearly as effective as full-length RGS4 in stimulating GTPase activity of $G\alpha_q$ (31). Consequently, upon cell stimulation the 4Box is recruited to signaling complexes to inhibit their activity and remains trapped in the complexes for as long as the cells are stimulated (see Ref. 27 for further details on the mode of action of the 4Box). We took advantage of the mode of interaction of the 4Box with GPCR signaling complexes to examine whether maximal activation of one GPCR type is sufficient to recruit 4Box to all GPCRs complexes, or stimulation of each GPCR complex is needed to inhibit signaling of the stimulated complex. Fig. 3, *B* and *C*, shows that stimulation of cells with 1 mM carbachol resulted in complete mobilization of the Ca^{2+} pool, as evident from the failure of 10 nM CCK8 and 100 nM bombesin (BS) to increase $[Ca^{2+}]_i$ in cells continuously stimulated with carbachol. When the cells were infused with 100 nM 4Box, stimulation with 1 mM carbachol resulted in a maximal initial signal that terminated rapidly and returned to base line at continuous stimulation with carbachol, due to receptor-dependent recruitment and trapping of 4Box (27). Fig. 3, *D* and *E*, shows that at continuous stimulation with carbachol the cells responded with a maximal signal to CCK8 (n = 15) and BS stimulation (n = 4). The response to CCK8 and BS had the same kinetics as that to carbachol, with a rapid onset and inhibition, and it remained inhibited for the duration of cell stimulation. This behavior is best explained if the various receptors are coupled to separate pools of cellular $G\alpha_q$ and PLCβ.

Polarized Expression of Ca^{2+} Signaling Proteins and Receptors—Polarized and restricted expression of Ca^{2+} channels and Ca^{2+} pumps in the luminal pole of epithelial cells appears to be important for initiation and propagation of polarized Ca^{2+} waves (7, 33). Co-immunoprecipitation of various Ca^{2+} signaling proteins indicates organization of the proteins into complexes in cellular microdomains (29). GPCRs are believed to be expressed mostly in the basal membrane. However, a recent report (34) suggested the possible expression of selective GPCRs next the luminal pole in rat goblet cells. With the development of selective antibodies that recognize several GPCRs, it was of interest to re-examine localization of GPCRs in pancreatic acini. Fig. 4 demonstrates the co-localization of the type 3 muscarinic (M3Rs) and CCK receptors (CCKRs) with Ca^{2+}-signaling proteins. Both receptors are expressed at high levels at the apical pole of pancreatic acini. Several antibodies used to localize the M3Rs revealed two cellular pools of these receptors, a plasma membrane and a Golgi-like pools. Double staining with pAb recognizing M3Rs and ZO1, a specific tight-junction protein (Fig. 4*A, top panels*), or IP_3R2 (not shown) showed that M3Rs localized in a non-uniform fashion with high levels at the lateral border, in close proximity or at the tight junctions, and low levels at the basal region (n = 10). However, the M35 and the 5H9 mAbs showed different patterns of localization. In permeabilized cells, the two mAbs showed strong labeling of an intracellular compartment and lower staining of the plasma membrane (n = 9 for M35, n = 6 for 5H9). This is particularly evident with the M35 mAb (Fig. 4, *lower middle panel*). The staining with this mAb was eliminated by adsorbing the mAb with recombinant M2Rs (Fig. 4, *lower left panel*), demonstrating specificity of the Abs. Because the 5H9 mAbs recognize an extracellular epitope evident of Sjögren syndrome (23), the plasma membrane staining was isolated by incubating intact cells with the Ab prior to cell fixation and permeabilization. Fig. 4*A, lower right panel*, shows that the M3Rs receptors are highly localized to the lateral membrane next to tight junctions (n = 4).

Selective localization was also observed with the CCKRs using two different pAbs recognizing different domains of the receptor, a pAb raised against amino acids 30–42 and a pAb raised against amino acids 411–429 of the type A CCKR (24). The two Abs specifically recognized recombinant and native CCKRs. Localization of the CCKRs at the apical pole of the lateral membrane (Fig. 4*B*) was similar to that of the M3Rs at the plasma membrane. The CCKRs at the plasma membrane were concentrated very near the IP_3R3 at the apical pole (n = 10). The anti-CCKRs Abs did not recognize a Golgi pool of this receptor.

Quantal Behavior and an All-or-None Ca^{2+} Release—The independence of the Ca^{2+} waves initiation site and propagation pattern of IP_3 concentration (Fig. 1) offered us the opportunity to examine whether local Ca^{2+} release is due to an all-or-none release from a compartmentalized pool (Fig. 5, *model A*) or a partial release from a continuous pool (Fig. 5, *model B*). The experiments used to distinguish between the two models and their predicted outcome according to each model are depicted in Fig. 5. Resting cells are in *state a*. Shortly after cell stimulation with submaximal agonist concentration (*state b*), all the Ca^{2+} is released from a sub-compartment of the pool (*model A*) or part of the Ca^{2+} is released from the entire pool (*model B*). At continuous stimulation (*state c*), high $[Ca^{2+}]_i$ at the mouth of the IP_3Rs reduces channel activity to allow partial reloading of the just discharged sub-pool with Ca^{2+} by the activated SERCA pumps (35) (*model A*). In this scenario, Ca^{2+} permeability of the sub-pool remains elevated, whereas Ca^{2+} permeability of the remaining pool is similar to that in resting cells. By con-

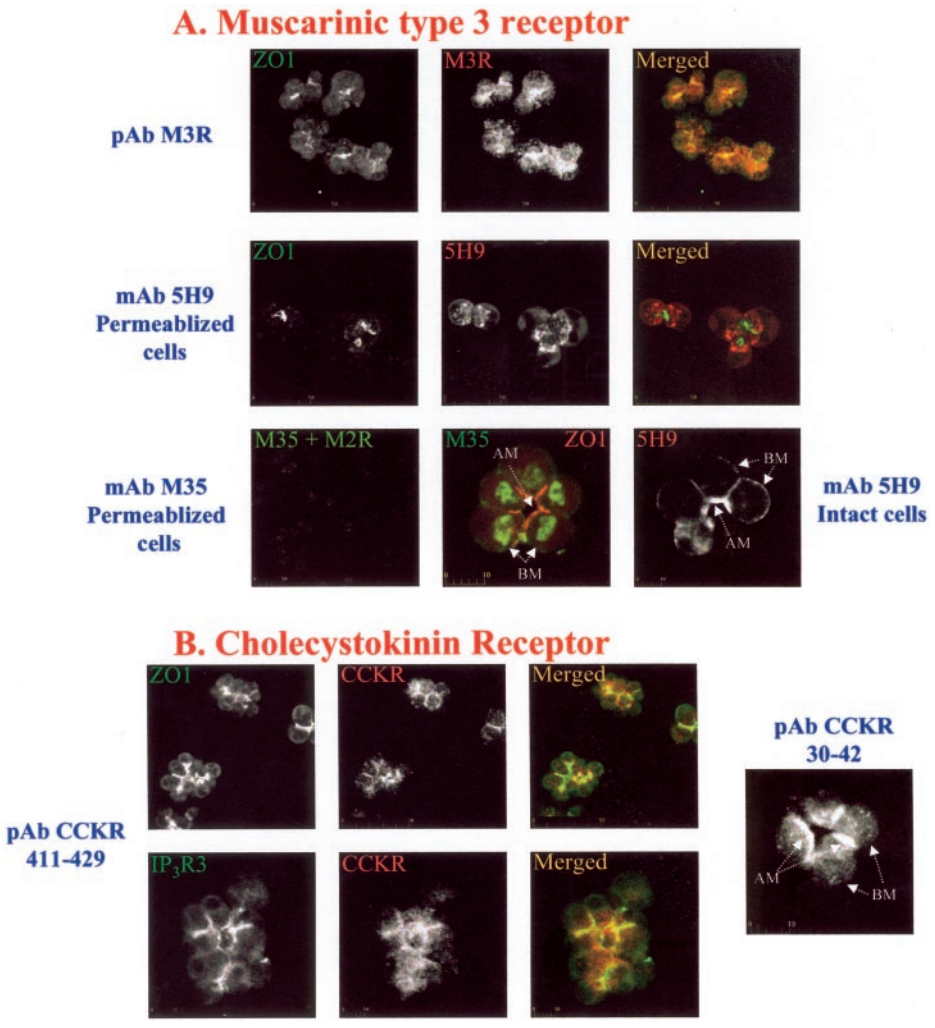

FIG. 4. **Polarized expression of GPCRs, ZO1, and IP_3Rs.** Isolated pancreatic acini were fixed and stained with the following Abs: *A*, *upper panels*, double staining with anti-ZO1 and anti-M3Rs; *middle panels*, double staining with anti-ZO1 and the anti-M3R mAb clone 5H9 after cell permeabilization; *lower left panel,* staining with the anti-muscarinic receptors mAb M35 pre-adsorbed with recombinant M2 receptors; *middle panels*, double staining with anti-M3Rs clone M35 and anti-ZO1; *lower right panel*, staining with anti-M3Rs mAb clone 5H9 in intact cells before permeabilization (see "Experimental Procedures"). *B, main panels,* double staining with anti-CCKRs raised against amino acids 411–429 of the CCKR and anti-ZO1 or anti-IP_3R2, as indicated; *right panel,* staining with an Ab that was raised against amino acids 30–42 of the CCKR.

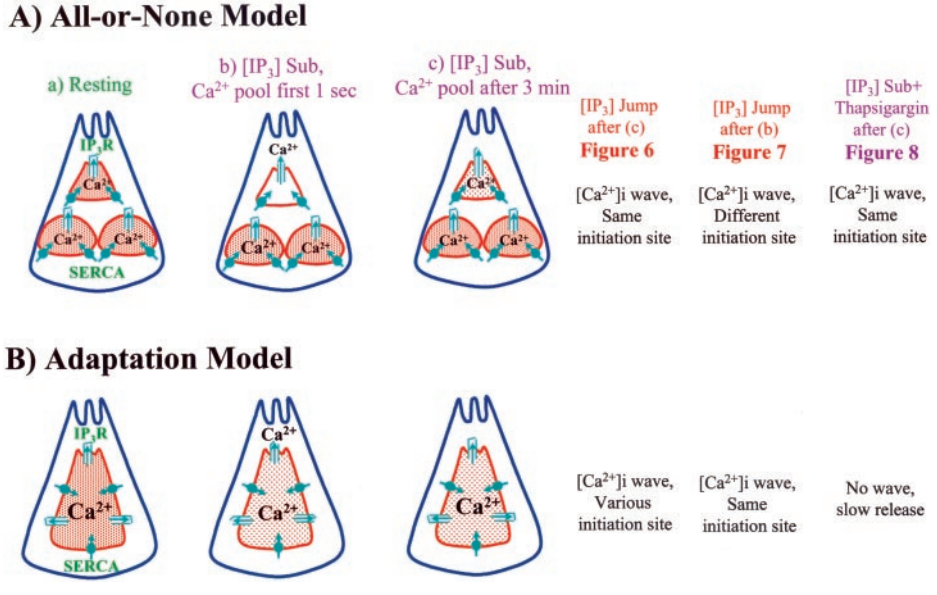

FIG. 5. **Models of quantal Ca^{2+} release.** *Model A* illustrates quantal Ca^{2+} release by an all-or-none mechanism and *model B* Ca^{2+} release by IP_3Rs adaptation mechanism. The text depicts the predicted outcomes of the agonist concentration jump and SERCA pump inhibition protocols by each model.

trast, *model B* assumes that at continuous stimulation, the activity of all the IP_3Rs channels is adapted to the lower Ca^{2+} content in the entire pool to terminate Ca^{2+} release so that Ca^{2+} permeability of the pool is similar to that of resting cells.

The first protocol we used is an agonist concentration jump after state c, long after return of [Ca^{2+}]$_i$ to near resting level. Model A predicts that the agonist (or IP_3) concentration jump will generate a Ca^{2+} wave with the same initiation site and pattern. Model B predicts generation of Ca^{2+} waves from random initiation sites and propagation pattern, because of the adaptation of the IP_3Rs that generated the first wave. Fig. 6 shows the results of such experiments with carbachol and CCK. It is clear that the Ca^{2+} waves initiated by low agonist and the concentration jump have the same initiation site and propaga-

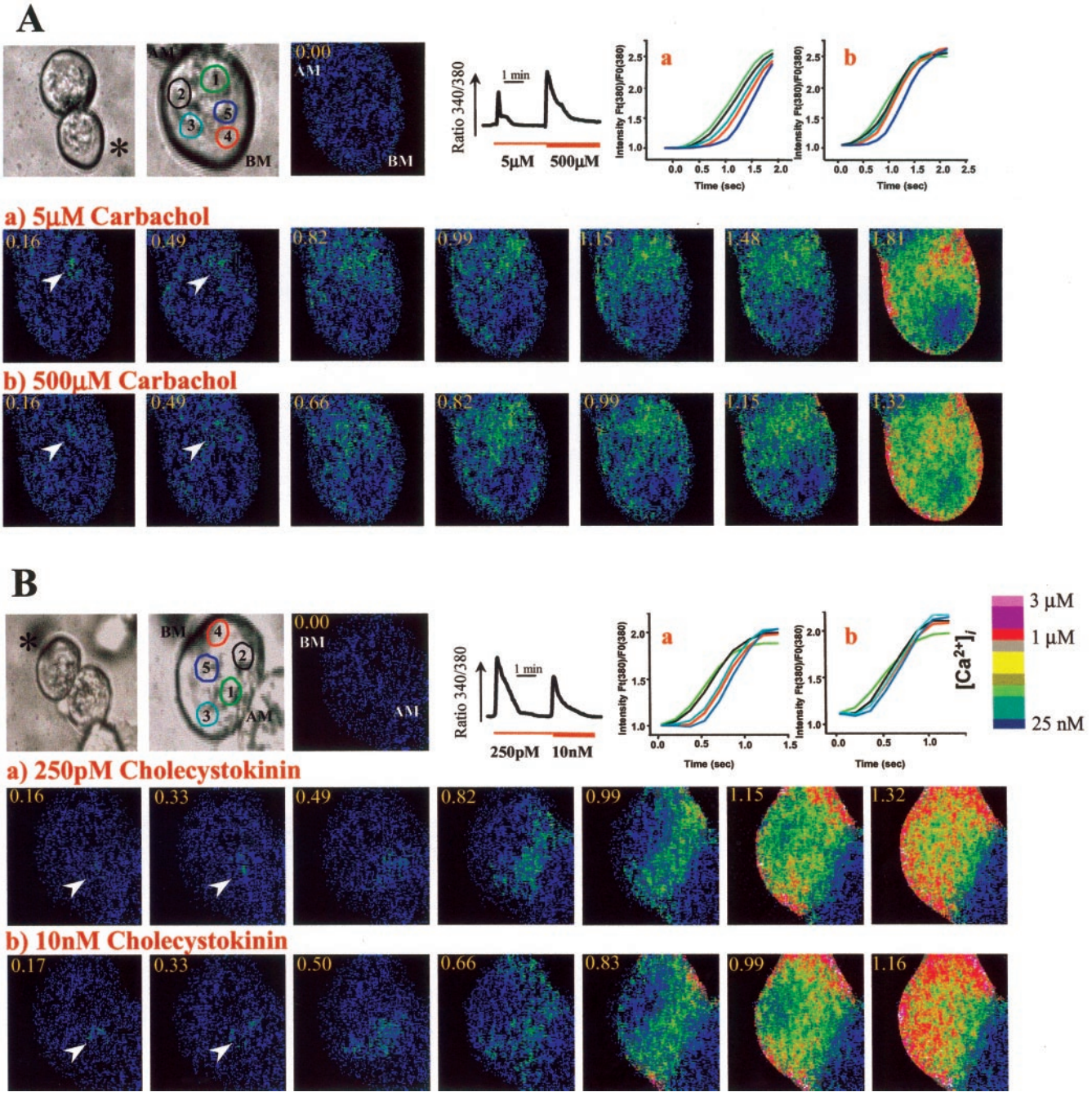

FIG. 6. **Successive stimulation by a delayed agonist concentration jump.** *A*, the cell was stimulated with 5 μM carbachol, and after return of Ca^{2+} to basal levels carbachol concentration was rapidly increased to 0.5 mM. *B*, the cell was stimulated with 0.25 nM CCK, and after return of Ca^{2+} to resting levels CCK concentration was increased to 10 nM. The *white arrowheads* show the Ca^{2+} wave initiation site for each stimulation period. Note the same initiation site by the low and high agonist concentrations in all experiments.

tion pattern. In five experiments with carbachol and four experiments with CCK, the average distances between the two initiation sites were 0.16 ± 0.03 and 0.10 ± 0.03 μm, respectively. Localized generation of IP_3 due to the polarized expression of the muscarinic receptors is likely to contribute to the constancy of the wave. Hence, in addition to testing the first prediction in Fig. 5, the constancy of the wave observed with the protocol of Fig. 6 lend further support for the autonomous behavior of signaling complexes

In the second protocol, the second Ca^{2+} wave was initiated by applying the concentration jump at the end of Ca^{2+} release evoked by the low agonist and before any reduction in $[Ca^{2+}]_i$ due to IP_3Rs channel adaptation. Model A predicts a second Ca^{2+} wave with different initiation site, due to discharge of all the Ca^{2+} from the pool mobilized by low agonist. Model B predicts a second Ca^{2+} wave from the same initiation site because Ca^{2+} is released prior to adaptation of the IP_3Rs activated by the first stimulus. The *trace* in Fig. 7 shows that this particular cell was exposed to the supermaximal concentration of 5 mM carbachol at 1.63 s after simulation with 5 μM carbachol. The concentration of 5 mM was used for the second stimulus, which was applied by rapid injection from a needle adjacent to the cell, to minimize the delay between agonist application and cell stimulation. The images in Fig. 7 show the results of four of five independent experiments with similar results. In contrast with the prediction of model B, but as predicted by model A, in all experiments the second Ca^{2+} wave evoked by the agonist concentration jump was initiated at a

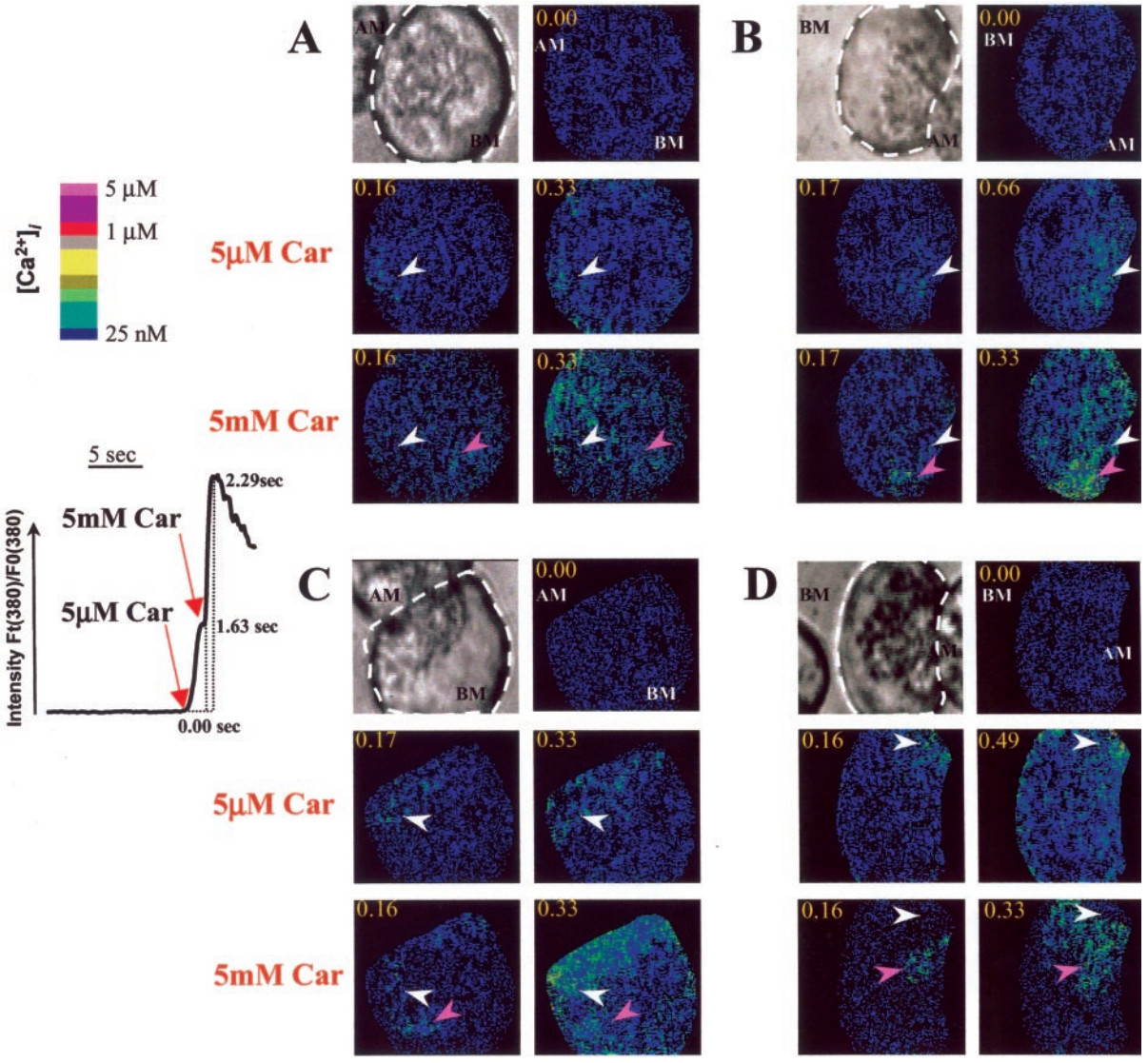

FIG. 7. **Successive stimulation by a rapid agonist concentration jump.** The *trace* shows the experimental protocol and the F_t/F_0 ratio of a typical experiment. The cells were stimulated with 5 mM carbachol at the peak of the $[Ca^{2+}]_i$ increase evoked by 5 μM carbachol. The images in *A–D* show the initiation site of the Ca^{2+} waves evoked by rapid, consecutive application of 5 μM (*white arrowhead*) and 5 mM carbachol (*magenta arrowhead*) to the same cells. Note the different initiation sites by the low and high agonist concentrations in all experiments.

different site than the first Ca^{2+} wave. The calculated distance between the initiation sites averaged 7.3 ± 1.3 μm (range 3.3–10.9 μm, $n = 5$), which is statistically different ($p < 0.01$) from the 0.19 ± 0.05 μm measured after delayed application of carbachol.

A shift in the initiation site of Ca^{2+} waves when the second wave was initiated at the end of the first Ca^{2+} release (Fig. 7) can be either because the initiation site still contained Ca^{2+} but the IP_3Rs at this site became refractory to a jump in IP_3 concentration, or because all the Ca^{2+} was released from this site by the first stimulus, and Ca^{2+} re-uptake is needed to initiate a second Ca^{2+} wave from the same site. The results in Fig. 8 provide direct evidence that Ca^{2+} release is an all-or-none process and that Ca^{2+} uptake must occur to initiate multiple Ca^{2+} waves from the same site. In these experiments we blocked the SERCA pumps with 10 μM thapsigargin (Tg) at different times after initiation of a Ca^{2+} wave. Model A predicts that inhibition SERCA pumps of cells continuously stimulated with low agonist at any time will trigger a Ca^{2+} wave with the same initiation site and pattern. Model B predicts that inhibition of SERCA pumps will not trigger a wave but rather will cause slow Ca^{2+} release because of adaptation of all IP_3Rs. Fig. 8*A* shows that in the absence of agonist stimulation, Tg caused a slow, peripheral to central Ca^{2+} release with no apparent Ca^{2+} wave or preferential release from any cellular region. As shown by the *trace* in Fig. 8*A*, $[Ca^{2+}]_i$ continued to increase for at least 30 s after exposure to Tg. Hence, in the absence of agonist stimulation Tg never initiated a Ca^{2+} wave.

Very different results were obtained when the cells were stimulated with submaximal agonist concentration and allowed to reduce $[Ca^{2+}]_i$ back to near basal level. As shown in Fig. 8*B*, under these conditions Tg evoked rapid, luminal to basal Ca^{2+} waves. Remarkably, in all experiments the Tg-evoked Ca^{2+} waves had the same initiation site and propagation pattern as the first Ca^{2+} wave evoked by the agonists. The distance between the initiation sites of the first waves evoked by carbachol and the second waves evoked by Tg in the same cells averaged 0.25 ± 0.1 μm ($n = 5$), which is not different from the 0.16 ± 0.03 μm measured with delayed concentration jump. The traces in *C* show that the magnitude of Ca^{2+} release by Tg was dependent on the incubation time with agonist. Thus, simultaneous stimulation of the cells with 5 μM carbachol and 10 μM Tg resulted in a rapid Ca^{2+} release but slow

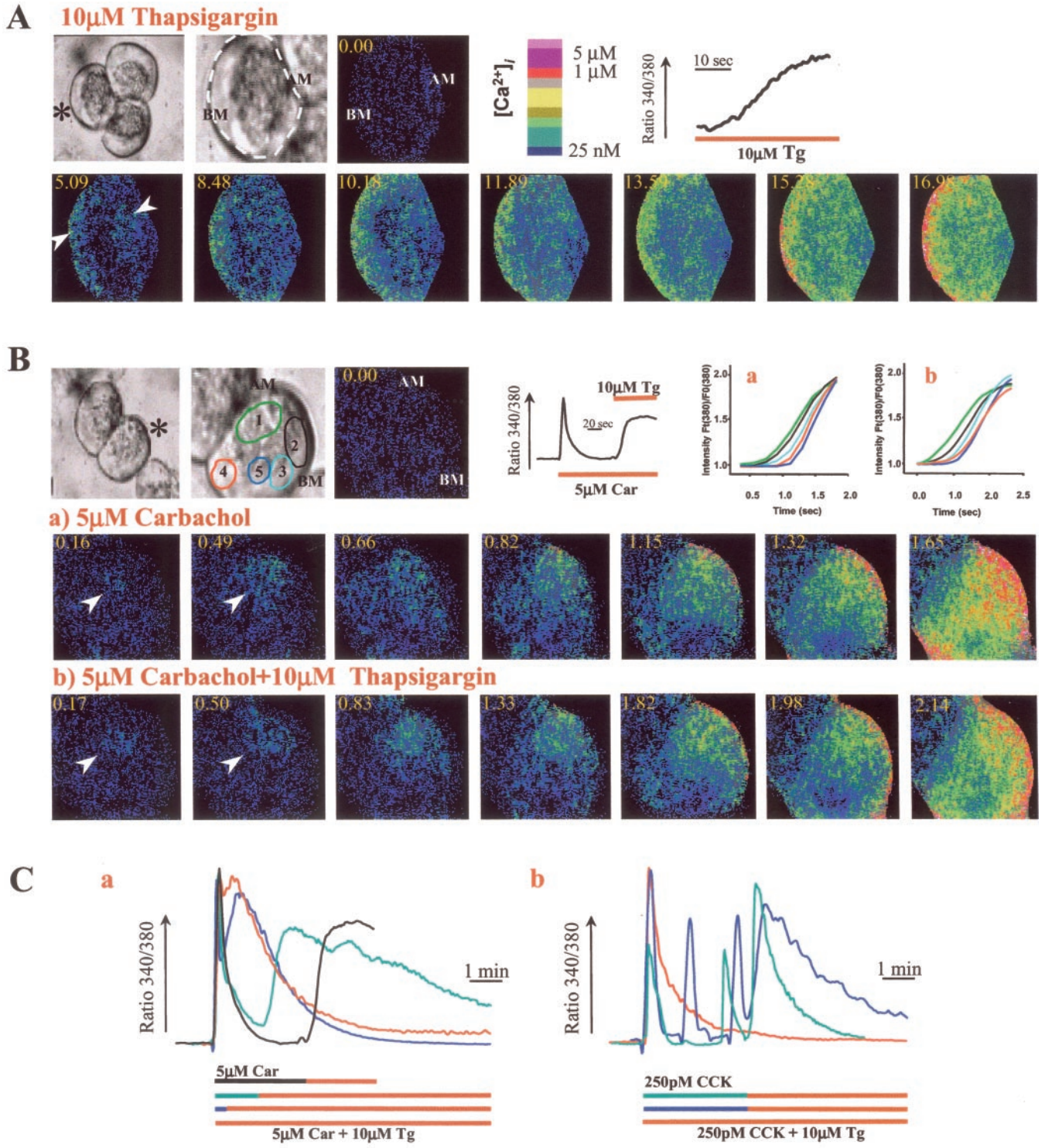

FIG. 8. **Ca^{2+} waves are evoked by inhibition of SERCA pumps in cells continuously stimulated with low agonist concentration.** *A,* maximal inhibition of SERCA pumps by 10 μM thapsigargin (*Tg*) in resting cells causes a slow peripheral to central Ca^{2+} release. *B,* maximal inhibition of SERCA pumps by Tg in cells continuously treated with 5 μM carbachol after return of $[Ca^{2+}]_i$ to basal level launch a Ca^{2+} wave with the same initiation site (*white arrowheads*) and propagation pattern as the initial wave evoked by carbachol. *C,* cells were stimulated with 5 μM carbachol (*a*) or 0.25 nM CCK (*b*). At different times during the reduction of $[Ca^{2+}]_i$ to basal levels, SERCA pumps were inhibited with 10 μM Tg. In all cases Tg evoked a rapid increase in $[Ca^{2+}]_i$ (in the form of a luminal-to-basal Ca^{2+} wave) with a subsequent slow reduction in $[Ca^{2+}]_i$.

return of $[Ca^{2+}]_i$ to basal levels, much slower than the rate observed with agonist alone (compare *red* to all other traces in *C*). Application of Tg at different times after cell stimulation caused a rapid increase in $[Ca^{2+}]_i$, to approximately the same level as that caused by the agonist and a slow reduction toward basal levels. Hence, Tg rapidly discharged only the Ca^{2+} that was incorporated into the initiation site during continuous stimulation and never to a level significantly higher than the initial level caused by the agonists. This behavior indicates that Ca^{2+} release from the initiation site must be an all-or-none process and that the initiation site reloads with Ca^{2+} during continuous stimulation with submaximal agonist concentration (model A). Furthermore, this behavior is incompatible with model B.

DISCUSSION

In the present work we addressed two important topics in Ca^{2+} signaling: how luminal to basal Ca^{2+} waves can be generated in a receptor-specific manner and whether quantal Ca^{2+} release reflects partial release from a continuous pool or an all-or-none release from a compartmentalized pool. Polarized exocrine cells are a good model system to address these questions because of the polarized nature of their Ca^{2+} signals (3), the polarized expression of high levels of Ca^{2+} transport proteins in the apical pole (7, 9, 29, 33, 36), and the generation of receptor-specific Ca^{2+} signals in these cells (6, 37). Our results indicate that signaling specificity in pancreatic acinar cells is aided by polarized expression and autonomous functioning of GPCRs and that quantal Ca^{2+} release is due to an all-or-none Ca^{2+} release from a compartmentalized Ca^{2+} pool.

Signaling specificity is a central topic in cell signaling (38). Several mechanisms have been shown to contribute to generation of specific GPCR-dependent Ca^{2+} signals, which include selective phosphorylation of IP_3Rs (39), differential couplings of Ca^{2+} release to Ca^{2+} entry (40), and different involvement of cADP-ribose and NADP-mediated Ca^{2+} release in the response (30). However, ultimately signaling specificity must reside in the communication between the receptor and downstream effectors. Indeed, RGS proteins function in a receptor-specific manner to confer receptor-specific signaling (41). Interaction of receptors with effectors requires their co-localization in cellular microdomains at sites of Ca^{2+} release. In polarized exocrine cells Ca^{2+} waves are always initiated at the apical pole. Whereas expression of all known IP_3R isoforms (7, 9), specific isoforms of SERCA pumps (33), and plasma membrane Ca^{2+} ATPase pumps (36) has been demonstrated, it remains a puzzle as to how IP_3 can be generated at this cellular microdomain because GPCRs are believed to reside largely at the basal pole. The localization of the M3Rs and CCKRs found at the present work clarifies this issue. The use of three anti-M3Rs and two anti-CCKRs, which recognize different epitopes, showed that both GPCR types are expressed at high level at close proximity or at the tight junctions. This localization removes the need to assume long range diffusion of IP_3 from the basal to the apical pole to initiate Ca^{2+} waves. Moreover, such localization of GPCRs is likely to contribute to the constancy of the Ca^{2+} waves generated by repetitive stimulation of the same GPCR complex.

In the present work we confirmed and extended the finding of receptor-specific Ca^{2+} waves by various GPCRs expressed in the same cell. By using the unique property of recruitment and trapping of the 4Box within signaling complexes (27), we demonstrated autonomous functioning of GPCRs. Furthermore, production of IP_3 by multiple GPCRs was nearly additive. The combined findings indicate that different GPCRs communicate with separate portions of the cellular pool of $G\alpha_q$ and $PLC\beta$ to generate IP_3 at separate cellular microdomains. The finding that the initiation site of Ca^{2+} waves was independent of IP_3 concentration, remaining constant when initiated by low (weak stimulation) or high IP_3 concentration (intense agonist stimulation), indicates that each GPCR communicates with a separate portion of the Ca^{2+} pool at the apical pole to generate Ca^{2+} waves with distinct initiation sites. Communication with a distinct portion of the Ca^{2+} pool may also reflect localized generation of IP_3 at the locus from which Ca^{2+} waves are initiated. Measurement of IP_3 in single pancreatic acinar cells is needed to test this point. At present, this is not feasible.

Since the discovery of the quantal behavior of Ca^{2+} release (15), two models were proposed as possible mechanisms of this phenomenon (see Fig. 5). The first model proposes that the intracellular Ca^{2+} pool is compartmentalized with respect to Ca^{2+} release, and the IP_3R Ca^{2+} release channels in the different compartments have variable affinity to IP_3 and Ca^{2+} release from individual compartments in an all-or-none process (15, 20). The second model proposed that the intracellular Ca^{2+} pool is continuous, and the affinity of all IP_3Rs to IP_3 is the same but is sensitive to Ca^{2+} content in the stores, and Ca^{2+} release is incremental due to rapid inactivating adaptation of the IP_3Rs (21). The evidence in favor of the adaptation model is the finding that stored Ca^{2+} regulates the affinity of the IP_3Rs for IP_3 in virtually all cell types examined (42), and a recent report (22) indicates that two rapid successive increases in IP_3 can liberate Ca^{2+} from the same site. The first evidence (42) is not mutually exclusive with the all-or-none model, and in the second case (22) rapid Ca^{2+} re-uptake into the stores was not prevented by inhibition of the SERCA pumps which, as shown in the present work, can explain the second Ca^{2+} release event.

Previous evidence in support of the all-or-none model was developed by measurement of Ca^{2+} permeability of the stores at increasing stimulus intensity (15). Increased agonist concentration mobilized a larger fraction of the Ca^{2+} pool. At persistent stimulation with submaximal agonist concentrations, Ca^{2+} permeability of the mobilized fraction of the pool remained very high, whereas Ca^{2+} permeability of the immobilized fraction remained very low, identical to that measured in resting cells (15). Another important finding in support of the all-or-none model is the variable sensitivity of IP_3 to Ca^{2+} release from different regions of pancreatic acinar cells (3, 11). The adaptation model predicts uniform IP_3 sensitivity throughout the cell.

In the present work we provide what we believe is strong evidence in support of the all-or-none model by first showing that the initiation site of Ca^{2+} waves is independent of IP_3 concentration. The implication of this finding is that there must exist a sub-pool that is more sensitive to IP_3 than the remaining cellular Ca^{2+} pool, and this pool is always discharged first upon cell stimulation. This provides additional evidence that the cellular Ca^{2+} pool is not uniform with respect to sensitivity to IP_3. Next, we used an agonist concentration jump to apply two consecutive rapid or delayed applications of IP_3. This protocol is equivalent to the two consecutive IP_3 application protocols used to conclude multiple Ca^{2+} release events from the same site (22). Two consecutive applications of IP_3 in pancreatic acini released Ca^{2+} from two separate sites when the second application was applied immediately at the end of Ca^{2+} release by the first application (Fig. 7). The difference between our results and those obtained in *Xenopus* oocytes (22) can be due to species differences or partial reloading of the just released pool with Ca^{2+}.

The adaptation model requires that at continued exposure to the same IP_3 concentration, the IP_3R channels adapt, becoming refractory to IP_3, and Ca^{2+} permeability of the pool is reduced back to resting level to terminate Ca^{2+} release. We used Tg to provide compelling evidence that this is not the case, at least in pancreatic acini. In fact, the Ca^{2+} pool liberated by submaximal receptor stimulation reloads with Ca^{2+} with continuous exposure to a constant agonist concentration. Furthermore, and most important, the Ca^{2+} permeability of the released and reloaded pool remains high, resulting in a Tg-evoked Ca^{2+} wave. The Tg-evoked Ca^{2+} wave had the same initiation site and propagation pattern as the Ca^{2+} wave evoked by the agonist (Fig. 8). Hence, the maintained high Ca^{2+} permeability of the liberated sub-pool, reloading of the sub-pool at continued stimulation, and the shift in the initiation site of Ca^{2+} wave observed at rapid agonist concentration jump are all compatible only with an all-or-non model of Ca^{2+} release. Therefore, we conclude that the principal mechanism behind the quantal

behavior of Ca^{2+} release is an all-or-none Ca^{2+} release from highly compartmentalized intracellular Ca^{2+} pool.

REFERENCES

1. Berridge, M. J. (1993) *Nature* **361,** 315–325
2. Rooney, T. A., Sass, E. J., and Thomas, A. P. (1990) *J. Biol. Chem.* **265,** 10792–10796
3. Kasai, H., Li, Y. X., and Miyashita, Y. (1993) *Cell* **74,** 669–677
4. Thorn, P., Lawrie, A. M., Smith, P. M., Gallacher, D. V., and Petersen, O. H. (1993) *Cell* **74,** 661–668
5. Nathanson, M. H., Fallon, M. B., Padfield, P. J., and Maranto, A. R. (1994) *J. Biol. Chem.* **269,** 4693–4696
6. Xu, X., Zeng, W., Diaz, J., and Muallem, S. (1996) *J. Biol. Chem.* **271,** 24684–24690
7. Lee, M. G., Xu, X., Zeng, W., Diaz, J., Wojcikiewicz, R. J., Kuo, T. H., Wuytack, F., Racymaekers, L., and Muallem, S. (1997) *J. Biol. Chem.* **272,** 15765–15770
8. Takemura, H., Yamashina, S., and Segawa, A. (1999) *Biochem. Biophys. Res. Commun.* **259,** 656–660
9. Yule, D. I., Ernst, S. A., Ohnishi, H., and Wojcikiewicz, R. J. (1997) *J. Biol. Chem.* **272,** 9093–9098
10. Ito, K., Miyashita, Y., and Kasai, H. (1999) *J. Cell Biol.* **146,** 405–413
11. Fogarty, K. E., Kidd, J. F., Tuft, D. A., and Thorn, P. (2000) *J. Physiol.* (*Lond.*) **526,** 515–526
12. Williams J. A., Groblewski, G. E., Ohnishi, H., and Yule, D. I. (1997) *Digestion* **58,** 42–45
13. Roettger, B. F., Rentsch, R. U., Hadac, E. M., Hellen, E. H., Burghardt, T. P., and Miller, L. J. (1995) *J. Cell Biol.* **130,** 579–590
14. Kasai, H., and Petersen, O. H. (1994) *Trends Neurosci.* **17,** 95–101
15. Muallem, S., Pandol, S. J., and Beeker, T. G. (1989) *J. Biol. Chem.* **264,** 205–212
16. Meyer, T., and Stryer, L. (1990) *Proc. Natl. Acad. Sci. U. S. A.* **87,** 3841–3845
17. Bootman, M. D., Berridge, M. J., and Taylor, C. W. (1992) *J. Physiol.* (*Lond.*) **450,** 163–178
18. Koizumi, S., Lipp, P., Berridge, M. J., and Bootman, M. D. (1999) *J. Biol. Chem.* **274,** 33327–33333
19. Totorici, G., Zhang, B.-X., Xu, X., and Muallem, S. (1994) *J. Biol. Chem.* **269,** 29621–29628
20. Taylor, C. W. (1992) *Adv. Second Messenger Phosphoprotein Res.* **26,** 109–142
21. Missiaen, L., Parys, J. B., De Smedt, H., and Oike, M., and Casteels, R. (1994) *Mol. Cell. Endocrinol.* **98,** 147–156
22. Callamaras, N., and Parker, I. (2000) *EMBO J.* **19,** 3608–3617
23. Nguyen, K. H., Brayer, J., Cha, S., Diggs, S., Yasunari, U., Hilal, G., Peck, A. B., and Humphreys-Beher, M. G. (2000) *Arthritis Rheum.* **43,** 2297–2306
24. Fischer de Toledo, C., Roettger, B. F., Morys-Wortmann, C., Schmidt, W. E., and Miller, L. J. (1997) *Am. J. Physiol.* **272,** G488–G497
25. Popov, S., Yu, K., Kozasa, T., and Wilkie, T. M. (1997) *Proc. Natl. Acad. Sci. U. S. A.* **94,** 7216–7220
26. Zeng, W., Xu, X., and Muallem, S. (1996) *J. Biol. Chem.* **271,** 18520–18526
27. Luo, X., Popov, S., Bera, A. M., Wilkie, T. M., and Muallem, S. (2001) *Mol. Cell* **7,** 651–660
28. Zhang, B. X., Tortorici, G., Xu, X., and Muallem, S. (1994) *J. Biol. Chem.* **269,** 17132–17135
29. Shin, D. M., Zhao, X. S., Zeng, W., Mozhayeva, M., and Muallem, S. (2000) *J. Cell Biol.* **150,** 1101–1112
30. Cancela, J. M., Gerasimenko, O. V., Gerasimenko, J. V., Tepikin, A. V., and Petersen, O. H. (2000) *EMBO J.* **19,** 2549–2557
31. Zeng, W., Xu, X., Popov, S., Mukhopadhyay, S., Chidiac, P., Swistok, J., Fisher, S. L., Ross, E. M., Muallem, S., and Wilkie, T. M. (1998) *J. Biol. Chem.* **273,** 34687–34690
32. Tesmer, J. J., Berman, D. M., Gilman, A. G., and Sprang, S. R. (1997) *Cell* **89,** 251–261
33. Lee, M. G., Xu, X., Zeng, W., Diaz, J., Kuo, T. H., Wuytack, F., Racymaekers, L., and Muallem, S. (1997) *J. Biol. Chem.* **272,** 15771–15776
34. Rios, J. D., Zoukhri, D., Rawe, I. M., Hodges, R. R., Zieske, J. D., and Dartt, D. A. (1999) *Ophthalmol. Vis. Sci.* **40,** 1102–1111
35. Muallem, S., Beeker, T. G., and Fimmel, C. J. (1987) *Biochem. Biophys. Res. Commun.* **149,** 213–220
36. Zhao, X.-S., Shin, D. M., Liu, L. H., Shull, G. E., and Muallem, S. (2001) *EMBO J.* **20,** 2680–2689
37. Yule, D. I., Lawrie, A. M., and Gallacher, D. V. (1991) *Cell Calcium* **12,** 145–151
38. Hunter, T. (2000) *Cell* **100,** 113–127
39. LeBeau, A. P., Yule, D. I., Groblewski, G. E., and Sneyd, J. (1999) *J. Gen. Physiol.* **113,** 851–872
40. Xu, X., Zeng, W., Diaz, J., Lau, K. S., Gukovskaya, A. C., Brown, R. J., Pandol, S. J., and Muallem, S. (1997) *Cell Calcium* **22,** 217–228
41. Xu, X., Zeng, W., Popov, S., Berman, D. M., Davignon, I., Yu, K., Yowe, D., Offermanns, S., Muallem, S., and Wilkie, T. M. (1999) *J. Biol. Chem.* **274,** 3549–3556
42. Missiaen, L., De Smedt, H., Droogmans, G., and Casteels, R. (1992) *Nature* **357,** 599–602